Single-Molecule Magnets

DOI: 10.1002/anie.201002690

An Octanuclear $[Cr^{III}_4Dy^{III}_4]$ 3d–4f Single-Molecule Magnet**

*Julia Rinck, Ghenadie Novitchi, Willem Van den Heuvel, Liviu Ungur, Yanhua Lan, Wolfgang Wernsdorfer, Christopher E. Anson, Liviu F. Chibotaru, and Annie K. Powell**

In memory of Ian J. Hewitt

Research on the synthesis, structures, and magnetic characterization of polynuclear coordination clusters containing anisotropic paramagnetic centers became an area of great importance in modern coordination chemistry since the discovery that such molecules can act as single-molecule magnets (SMMs).[1] The fundamental characteristic of SMM behavior is the presence of an energy barrier to the reorientation of the spin of the ground state and this can be defined in terms of a large (or at least nonzero) ground spin state (S) and a large magnetic anisotropy of the Ising (easy axis) type with a negative zero-field splitting parameter, D. Coordination clusters containing the Mn^{III} ion are the richest source of SMMs largely as a result of its favorable Ising anisotropy. In particular, Mn_{12}Ac and related carboxylate systems[1,2a] provided the first examples of SMMs, whilst the recently reported Mn_6 oxime series includes examples with the highest energy barriers so far reported.[2b] It has been recognized that lanthanide ions also represent a rich source of highly anisotropic spin carriers;[3] therefore, in the quest for new SMMs attention has recently focused on incorporating such highly anisotropic 4f ions into 3d systems.[4–8] Initially, much work concentrated on mixing 4f ions with Mn^{III}. However, experience shows that relatively isotropic ions can also be used to help aggregate 3d–4f clusters in such a way as to produce new examples of SMMs often with enhanced SMM properties compared with the pure 3d analogues. Here we report a new SMM with a 4f-square in a 3d-square (more correctly butterfly) topology, which illustrates that mixing highly anisotropic 4f ions (here Dy^{III}) with the isotropic $3d^3$ ion Cr^{3+} leads to a system in which the 3d ion pins the spin topology of the 4f ions giving rise to fascinating magnetic properties.

Reaction of methyldiethanolamine (H_2mdea) and NaN_3 with chromium(II) chloride in acetonitrile, under an inert atmosphere, followed by addition of $Dy(NO_3)_3{\cdot}6H_2O$, pivalic acid (HPiv), and dichloromethane and exposure to air gave pink crystals of $[Cr_4Dy_4(\mu_3\text{-}OH)_4(\mu\text{-}N_3)_4(mdea)_4(piv)_4]{\cdot}3CH_2Cl_2$ (**1**), which crystallizes in the tetragonal space group $I\bar{4}2m$ with $Z=2$. The complex has $\bar{4}2m$ site symmetry and its structure is shown in Figure 1.

The central core of the aggregate is based on a perfect square of four Dy cations with Dy···Dy distances of 4.0339(2) Å. Each pair of adjacent Dy centers is bridged by a (μ_3-OH) ligand to a Cr^{III} cation with Cr(1)–O(1) 1.970(3), Dy(1)–O(1) 2.407(2), and Cr···Dy 3.3333(4) Å. The four Cr centers are displaced alternately above and below the Dy_4 square by 1.3998(6) Å, so that the apparent "Dy_4-square-within-a-Cr_4-square" description of the $Cr_4Dy_4(\mu_3\text{-}OH)_4$ unit when viewed down the fourfold axis actually corresponds to a square within a butterfly motif. Each Dy···Dy edge is also bridged by an end-on azide ligand that is on the opposite face of the Dy_4 square to the corresponding (μ_3-OH) bridge. Cr(1) is chelated by a doubly-deprotonated $(mdea)^{2-}$ ligand with the nitrogen atom *trans* to the (μ_3-OH) ligand and the two oxygen atoms forming bridges to the adjacent dysprosium atoms. The coordination shell of the aggregate is completed by eight pivalate ligands, each forming a *syn*,*syn*-bridge between adjacent Cr^{III} and Dy^{III} centers around the periphery of the complex. Since the Dy anisotropies lie perpendicular to the twofold axes running through the respective Dy centers, the magnetic symmetry (C_{2v}) is now lower than the molecular site symmetry (D_{2d}), and the polar magnetic point group results in a nonzero tensor sum of the individual anisotropies.

The $\chi_M T$ product versus temperature plot for **1** under an applied magnetic field of 0.1 T is shown in Figure 2. The χT product at room temperature is 64.23 $cm^3\,K\,mol^{-1}$, which is in good agreement with the expected value of 64.18 $cm^3\,K\,mol^{-1}$, for four Cr^{III} ($S=3/2$, $g=2$, $C=1.875$ $cm^3\,K\,mol^{-1}$) and four Dy^{III} ions ($S=5/2$, $L=5$, $^6H_{15/2}$, $g=4/3$, $C=14.17$ $cm^3\,K\,mol^{-1}$).[3] On lowering the temperature, the χT product at 1000 Oe decreases steadily until it reaches 80 K

[*] J. Rinck, Dr. G. Novitchi, Dr. Y. Lan, Dr. C. E. Anson, Prof. Dr. A. K. Powell
Institute of Inorganic Chemistry
Karlsruhe Institute of Technology
Engesserstrasse 15, 76131 Karlsruhe (Germany)
Fax: (+49) 721-608-8142
E-mail: annie.powell@kit.edu
W. Van den Heuvel, L. Ungur, Prof. Dr. L. F. Chibotaru
Division of Quantum and Physical Chemistry and
INPAC—Institute of Nanoscale Physics and Chemistry
Katholieke Universiteit Leuven
Celestijnenlaan 200F, 3001 Heverlee (Belgium)
L. Ungur
INPAC—Institute for Nanoscale Physics and Chemistry
Katholieke Universiteit Leuven
Celestijnaniaan 200F, 3001 Heverlee (Belgium)
Prof. Dr. W. Wernsdorfer
Institut Néel—CNRS, BP 166
25 Avenue des Martyrs
38042 Grenoble Cedex 9 (France)

[**] We thank the DFG Center for Functional Nanostructures (CFN), EU FP6 MAGMANet NoE, Alexander von Humboldt Stiftung (G.N.), INPAC (K.U. Leuven), and the Flemish Fund for Scientific Research (FWO) for financial support.

Supporting information for this article is available on the WWW under http://dx.doi.org/10.1002/anie.201002690.

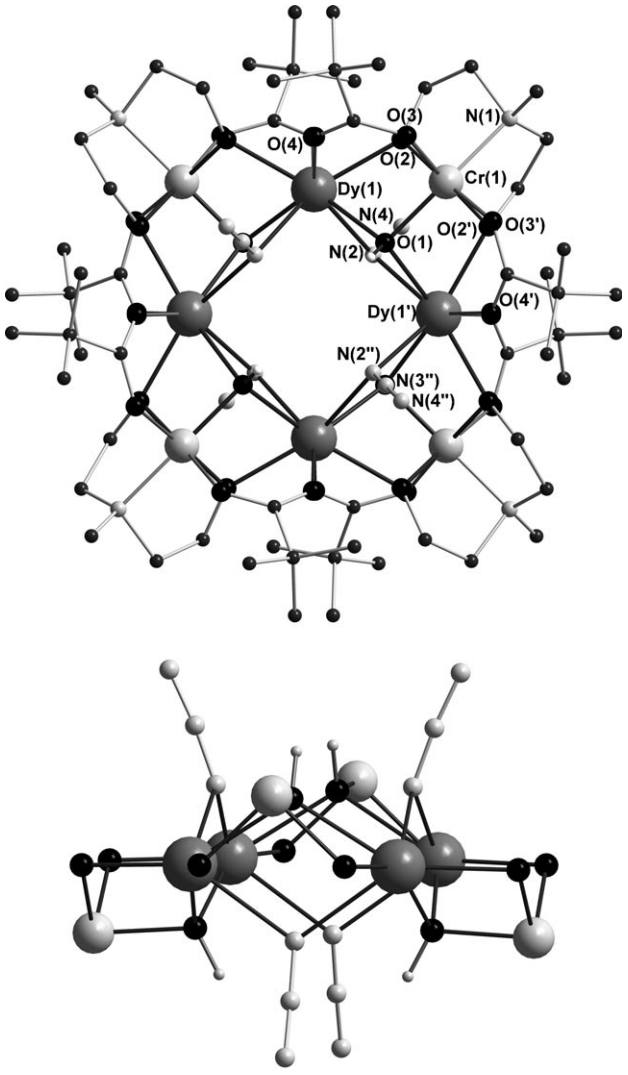

Figure 1. Top: Molecular structure of **1**, disordered atoms and organic H atoms have been omitted for clarity. Bottom: The aggregate core showing deviations of the Cr atoms out of the Dy_4 plane.

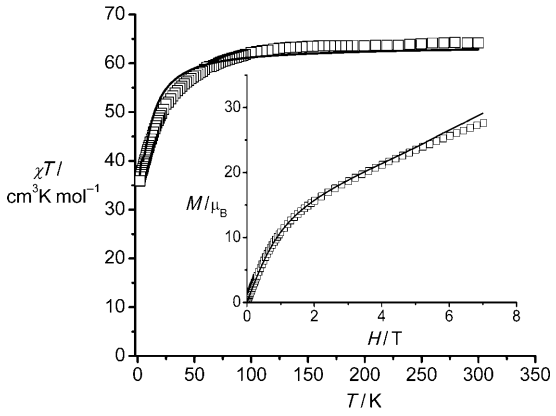

Figure 2. Temperature dependence of χT under a 0.1 T applied field for **1** (squares) compared with that calculated (basis set 1) by using the parameters in the text. Inset: Experimental field dependence of magnetization at 2 K (squares) compared to the calculated curve.

and then drops rapidly to reach a minimum value of 35.9 $cm^3 K mol^{-1}$ at 1.8 K. This behavior indicates the presence of intramolecular antiferromagnetic interactions amongst the spin carriers but from these results alone we cannot dismiss the possibility that this behavior partially or totally originates from the thermal depopulation of the Dy^{III} excited states (Stark sublevels of the $^6H_{15/2}$ state).[3a] The field dependence of the magnetization at low temperatures shows an initial rapid increase for fields up to 2 T, reaching 16.4 μ_B, followed by a slower quasi-linear increase up to 7 T, when it reaches 28.9 μ_B (Figure 2 inset). This linearity at $B > 2$ T may be a peculiarity of the powder magnetization as illustrated in the ab initio calculation, but the non-superposed magnetization curves at different temperatures (see Figure S1 in the Supporting Information) might also suggest the presence of magnetic anisotropy and/or the population of low-lying excited states.

The relaxation of the magnetization has been investigated using AC susceptibility measurements as a function of temperature at different frequencies and also at different temperatures as a function of frequency (see Figure S2 and S3 in the Supporting Information). Compound **1** clearly exhibits slow relaxation of its magnetization below 5 K, as in a zero-dc field strong frequency-dependent in-phase and out-of-phase signals are observed. The maximum of the out-of-phase signal was observed at 2.2 K at a frequency of 1500 Hz. The shape and frequency dependence of this feature strongly suggests that compound **1** is a SMM. To confirm SMM behavior the magnetizations of single crystals of **1** as a function of applied field were studied with a micro-SQUID array in the 0.04–1.1 K range.[9] The measurements at 0.04 K revealed the presence of hysteresis loops (0.2 T; Figure 4a).

The AC susceptibility of the complex may be expressed by using the Cole–Cole equations[10] (Figure 3 insert). The best fits of the in-phase versus out-of-phase susceptibility in the range of 1.9–2.2 K was obtained with $\alpha = 0.42$–0.5 (see Figure S3 in the Supporting Information). The relatively high value of α indicates that more than one relaxation process operates under these conditions. AC susceptibilities were also measured with the application of a small DC field. The relaxation is almost unchanged, suggesting that the relaxation mechanism of this SMM, at least above 1.8 K, is not influenced by quantum effects. The characteristic relax-

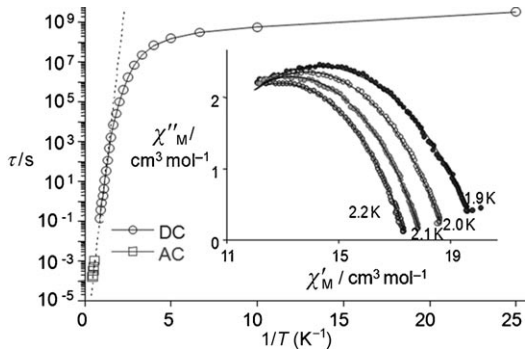

Figure 3. Arrhenius plot constructed by using AC χ_M'' and DC decay data (Figure S5), and Cole–Cole plot ($\alpha = 0.42$–0.5) at the indicated temperatures (inset).

ation time (τ) of the system was extracted from the frequency-sweeping data at different temperatures (Figure 3) and was found to follow a thermally activated Arrhenius law with the energy gap Δ estimated at 15 K and the preexponential factor τ_0 $1.9(1)\times10^{-7}$ s.

Ab initio calculations for the dysprosium and chromium fragments were performed by using a CASSCF/CASPT2 approach that includes the spin–orbit coupling,[11] and their magnetic properties simulated by the approach recently developed by some of us[12] with two basis sets (see the Supporting Information). In the basis set 1 the Dy^{III} ions are found to be highly anisotropic with $g_{\parallel} > 19.67$ and $g_{\perp} \approx 0$ in the ground Kramers doublet. The direction of anisotropy axes (shown in Figure S8a by red dashed lines) lie in the planes perpendicular to the twofold axes passing through the corresponding dysprosium ions (see Figure S8b in the Supporting Information).[13] On the contrary, the Cr^{III} ions are almost isotropic with $g \approx 1.97$ (Table S3). The ground Kramers doublet on each dysprosium ion is separated from the first excited one by approximately 30 cm^{-1} (see Table S1 in the Supporting Information). Therefore for the description of low-lying exchange multiplets of the whole Cr_4Dy_4 complex we consider that only the ground Kramers doublet of each Dy^{III} is involved in the exchange interaction. The high value of $g_{\parallel}$ on the dysprosium ions is proof of the essentially axial nature of the ground Kramers doublet,[14a] therefore, the exchange interaction amongst Dy^{III} centers and with neighboring chromium ions will be close to an Ising type[14b,c] (see [Eq. (S1)] in the Supporting Information). In the frame of this model we can simulate satisfactorily the powder magnetic data (Figure S9). However the feature that looks like an extended magnetization step in the low-temperature magnetization loops (Figure 4b), in the lower branch for negative fields and in the upper branch for positive fields, cannot be reproduced for any parameters of the Ising model, even by including the Heisenberg interaction between neighboring Cr ions.

Therefore we repeated the ab initio calculations for the Dy^{III} fragment with an enlarged basis set (2 in the Supporting Information) and found that the ground Kramers doublet is much less anisotropic than in the previous calculation ($g_x = 1.7$, $g_y = 5.8$, $g_z = 14.4$). The main anisotropy axes (g_z) on the dysprosium sites are shown in Figure 5 by red dashed lines. Such sensitivity of calculated g factors and the directions of anisotropy axes (Table S1) on the basis set has not been observed for other dysprosium compounds, for example, Dy^{III} triangles,[12b] and is probably due to a much closer spacing of excited Kramers doublets in the present case (see Table S1). The thus obtained less axial anisotropy of the ground Kramers doublet on the dysprosium sites implies a more general form of anisotropic exchange interaction and, importantly, not exclusively of Ising type anymore for the Dy–Cr and Dy–Dy pairs. We treated these anisotropic exchange interactions within the Lines model as described elsewhere,[12] including one exchange parameter for each coupled pair of metal atoms, that is, J_1, J_2, and J_3 for the Dy–Cr, Dy–Dy, and Cr–Cr pairs, respectively. Figure 2 shows the calculated χT and $M(H)$ for a powder for the set $J_1 = -4.5$ cm^{-1}, $J_2 = 5.0$ cm^{-1}, and $J_3 = -0.55$ cm^{-1} where each Dy^{III} ion is described as $S = 1/2$. We can see that the calculations reproduce the steep increase and the lack of saturation of magnetization up to $H = 7$ T. Furthermore, the calculations prove that the linear

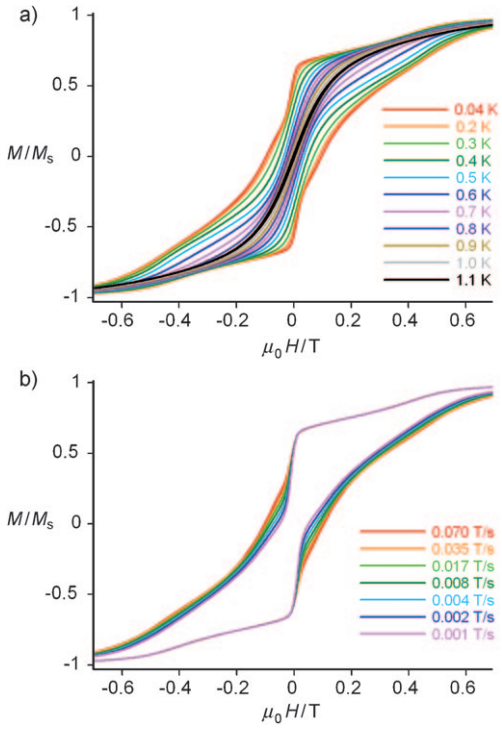

Figure 4. Plot of normalized magnetization (M/M_s) versus applied field ($\mu_o H$). The loops are shown at different temperatures at 0.035 Ts^{-1} (a) and at different sweep rates at 0.04 K (b).

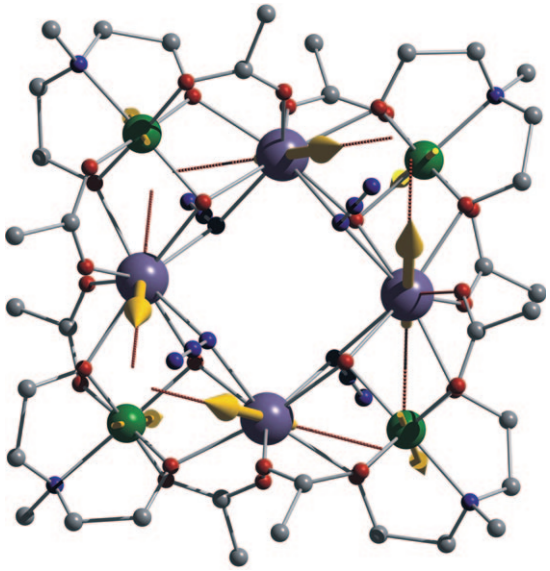

Figure 5. Directions of main anisotropy axes on Dy^{III} (dashed lines) and the direction of magnetic moments (arrows) in the ground state of the complex with saturated magnetization along the main anisotropy axis, perpendicular to the Dy_4 plane. Note a small deviation of magnetic moments on Dy^{III} ions from the corresponding main anisotropy axes.

behavior of $M(H)$ at $H > 1$ T only arises for a powder and not in a single crystal.

Figure 6b shows the calculated magnetization as a function of the magnetic field applied in the direction of the S_4 axis of the complex (Z). We can see that the feature looking like an extended magnetization step at $T = 0.04$ K in Figure 4b is qualitatively reproduced. Calculations at $T = 0$ K (black line

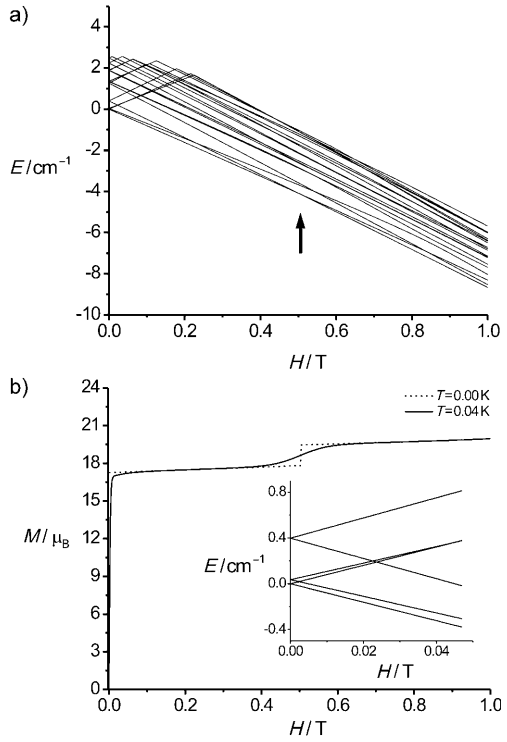

Figure 6. Evolution of the lowest energy levels (a) and of the molar magnetization (b) with the magnetic field applied along the main anisotropy axis of **1**. The inset in (b) shows the enlarged domain of the diagram in (a) around the ground state.

in Figure 6b) reveal the presence of one magnetization step responsible for this feature, which arises due to a ground state level crossing at $H = 0.5$ T (vertical arrow in Figure 6a). The last feature is actually an avoided crossing, becoming more pronounced (and the magnetization steps in Figure 6b more extended) if the applied field is not parallel to the main anisotropy axis Z, which would be the case if the sample was not perfectly aligned. We should note that the set of exchange parameters used in the above simulations is not the only one possible. Figure S10 and S11 show similar simulations for smaller exchange parameters, where the amplitude of the jump of magnetization of the extended-step-like feature (see Figure S11b in the Supporting Information) is obtained closer to the experimental value (Figure 4b). The increase of this amplitude is due to several avoided crossings arising now in the ground state (Figure S11a). The reason for the appearance of one or several ground state crossings in a narrow interval of fields is the existence of frustrated exchange interactions in the pairs Dy–Cr and Cr–Cr provided by the chosen exchange parameters. The relatively large avoided crossings of the ground state level are the reason for the independence of the lower branch of magnetization curves for negative fields (upper branch for positive field) from the field sweep rate (Figure 4b).

In contrast, the crossing of the lowest states in the zero-field point (Figure 6b, inset) is practically not avoided. The ground state of the complex is an Ising doublet composed of two energy levels belonging to the A_1 and A_2 rreducible representations of the D_{2d} group and separated by a tunneling gap of 1.7×10^{-6} cm^{-1} according to our calculations.[15] The corresponding tunneling states are even and odd combinations, respectively, of the two components of the Kramers doublet, shown in Figure 5, and the time-reversed component. Furthermore, the g tensor is calculated to be very anisotropic, with $g_Z = 34.5$ and $g_\perp = 0$ ($< 1.0 \times 10^{-13}$), which means that transverse components of the magnetic field present in the crystal will not be efficient for the reorientation of magnetization. This can be compared with the situation in the $Co^{II}{}_3Co^{III}{}_4$ wheel where $g_\perp > 0.1$,[12a] and this explains why the latter is not a SMM. These two factors are in line with the observed SMM behavior of **1**.

In conclusion, we have synthesized the first heterometallic Cr–Dy single-molecule magnet with an energy barrier to spin reorientation of 15 K. The anisotropy in this octanuclear compound, from which its SMM behavior originates, is of axial type and results from strong magnetic anisotropy on four Dy^{III} ions. Noteworthy here is the presence of the competing Dy–Cr, Dy–Dy, and Cr–Cr exchange interactions, which govern the spin structure. These lead to the low-lying features of the energy spectrum of exchange multiplets and avoided energy level crossings, allowing resonant tunneling between those levels, manifested by magnetization steps and field sweep rate-dependent hysteresis.

Experimental Section

Crystal data for **1**: $C_{63}H_{126}Cl_6Cr_4Dy_4N_{16}O_{28}$, 2626.50 g mol^{-1}, pink block, tetragonal, $I\bar{4}2m$, $T = 100$ K, $a = 19.3300(8)$, $c = 13.6488(11)$ Å, $V = 5099.9(5)$ Å^3, $Z = 2$, $\rho_{calcd} = 1.710$ Mg m^{-3}, $F(000) = 2604$, $\mu(Mo_{K\alpha}) = 3.530$ mm^{-1}; 17801 data measured, 3088 unique ($R_{int} = 0.0174$); $wR_2 = 0.0462$, $S = 1.052$ (all data, 192 parameters, 21 restraints), $R_1 = 0.0178$ (3025 data with $I > 2\sigma(I)$), largest final difference peak/hole $+0.74/-0.52$ e Å^{-3}. CCDC-749296 contains the supplementary crystallographic data for this paper. These data can be obtained free of charge from The Cambridge Crystallographic Data Centre via www.ccdc.cam.ac.uk/data_request/cif. For further details of the refinement see the Supporting Information.

Magnetic measurements were obtained with a Quantum Design SQUID magnetometer MPMS-XL in the range of 1.8 to 300 K with DC applied fields ranging from 0 to 7 T. The measurements were performed on a polycrystalline sample of 8.6 mg dispersed in Apiezon grease of 5.8 mg. AC susceptibility measurements were obtained by applying an oscillating AC field of 3 Oe and frequencies ranging from 1 to 1500 Hz. M versus H measurements were performed at 100 K to check for the presence of ferromagnetic impurities, which were found to be absent. The magnetic data were corrected for the sample holder and the diamagnetic contribution.

Received: May 4, 2010
Published online: September 2, 2010

Keywords: anisotropy · chromium · lanthanides · magnetic properties · single-molecule magnets

[1] a) D. Gatteschi, R. Sessoli, *Angew. Chem.* **2003**, *115*, 278; *Angew. Chem. Int. Ed.* **2003**, *42*, 268; b) G. Christou, D. Gatteschi, D. N. Hendrickson, R. Sessoli, *MRS Bull.* **2000**, *25*, 66.

[2] a) T. Lis, *Acta Crystallogr. Sect. B* **1980**, *36*, 2042; b) T. C. Stamatatos, K. A. Abboud, W. Wernsdorfer, G. Christou, *Angew. Chem.* **2008**, *120*, 6796; *Angew. Chem. Int. Ed.* **2008**, *47*, 6694; c) T. C. Stamatatos, K. A. Abboud, W. Wernsdorfer, G. Christou, *Angew. Chem.* **2007**, *119*, 902; *Angew. Chem. Int. Ed.* **2007**, *46*, 884.

[3] a) D. Gatteschi, C. Benelli, *Chem. Rev.* **2002**, *102*, 2369; b) R. Sessoli, A. K. Powell, *Coord. Chem. Rev.* **2009**, *253*, 2328.

[4] a) G. Novitchi, W. Wernsdorfer, L. F. Chibotaru, J.-P. Costes, C. E. Anson, A. K. Powell, *Angew. Chem.* **2009**, *121*, 1642 – 1647; *Angew. Chem. Int. Ed.* **2009**, *48*, 1614 – 1619; b) J.-P. Costes, F. Dahan, W. Wernsdorfer, *Inorg. Chem.* **2006**, *45*, 5; c) F. Mori, T. Nyui, T. Ishida, T. Nogami, K.-Y. Choi, H. Nojiri, *J. Am. Chem. Soc.* **2006**, *128*, 1440; d) S. Osa, T. Kido, N. Matsumoto, N. Re, A. Pochaba, J. Mrozinski, *J. Am. Chem. Soc.* **2004**, *126*, 420; e) C. Aronica, G. Pilet, G. Chastanet, W. Wernsdorfer, J.-F. Jacquot, D. Luneau, *Angew. Chem.* **2006**, *118*, 4775; *Angew. Chem. Int. Ed.* **2006**, *45*, 4659; f) G. Novitchi, J.-P. Costes, J.-P. Tuchagues, L. Vendier, W. Wernsdorfer, *New J. Chem.* **2008**, *32*, 197.

[5] V. Chandrasekhar, B. M. Pandian, R. Boomishankar, A. Steiner, J. J. Vittal, A. Houri, R. Clérac, *Inorg. Chem.* **2008**, *47*, 4918.

[6] V. Chandrasekhar, B. M. Pandian, R. Boomishankar, A. Steiner, J. J. Vittal, A. Houri, R. Clérac, *Inorg. Chem.* **2009**, *48*, 1148.

[7] a) M. Ferbinteanu, T. Kajiwara, K-Y. Choi, H. Nojiri, A. Nakamoto, N. Kojima, F. Cimpoesu, Y. Fujimura, S. Takaishi, M. Yamashita, *J. Am. Chem. Soc.* **2006**, *128*, 9008; b) M. Murugesu, A. Mishra, W. Wernsdorfer, K. Abboud, G. Christou, *Polyhedron* **2006**, *25*, 613; c) F. Pointillart, K. Bernot, R. Sessoli, D. Gatteschi, *Chem. Eur. J.* **2007**, *13*, 1602.

[8] a) V. Mereacre, A. M. Ako, R. Clérac, W. Wernsdorfer, G. Filoti, J. J. Bartolomé, C. E. Anson, A. K. Powell, *J. Am. Chem. Soc.* **2007**, *129*, 9248; b) V. Mereacre, A. M. Ako, R. Clérac, W. Wernsdorfer, I. J. Hewitt, C. E. Anson, A. K. Powell, *Chem. Eur. J.* **2008**, *14*, 707; c) M. N. Akhtar, Y. Lan, V. Mereacre, R. Clérac, C. E. Anson, A. K. Powell, *Polyhedron* **2009**, *28*, 1698; d) C. Zaleski, E. Depperman, J. Kampf, M. Kirk, V. Pecoraro, *Angew. Chem.* **2004**, *116*, 4002; *Angew. Chem. Int. Ed.* **2004**, *43*, 3912; e) A. Mishra, W. Wernsdorfer, K. Abboud, G. Christou, *J. Am. Chem. Soc.* **2004**, *126*, 15648; f) A. Mishra, W. Wernsdorfer, S. Parsons, G. Christou, E. Brechin, *Chem. Commun.* **2005**, 2086.

[9] W. Wernsdorfer, *Adv. Chem. Phys.* **2001**, *118*, 99.

[10] a) D. Gatteschi, R. Sessoli, J. Villain, *Molecular Nanomagnets*, Oxford University Press, Oxford, **2006**; b) K. S. Cole, R. H. Cole, *J. Chem. Phys.* **1941**, *9*, 341.

[11] G. Karlström, R. Lindh, P. Å. Malmqvist, B. O. Roos, U. Ryde, V. Veryazov, P. O. Widmark, M. Cossi, B. Schimmelpfennig, P. Neograd y, L. Seijo, *Comput. Mater. Sci.* **2003**, *28*, 222.

[12] a) L. F. Chibotaru, L. Ungur, C. Aronica, H. Elmoll, G. Pilet, D. Luneau, *J. Am. Chem. Soc.* **2008**, *130*, 12445 – 12455; b) L. Ungur, W. Van den Heuvel, L. F. Chibotaru, *New J. Chem.* **2009**, *33*, 1224 – 1230.

[13] Because the site symmetry of each dysprosium ion is C_2 the main magnetic axis can either lie along this rotational axis or in the perpendicular plane.

[14] a) W. Van den Heuvel, L. F. Chibotaru, unpublished; b) A. Soncini, L. F. Chibotaru, *Phys. Rev. B* **2008**, *77*, 220406; c) D. Visinescu, A. M. Madalan, M. Andruh, C. Duhayon, J.-P. Sutter, L. Ungur, W. Van den Heuvel, L. F. Chibotaru, *Chem. Eur. J.* **2009**, *15*, 11808.

[15] Exactly the same situation (with a smaller tunneling gap) takes place in the Mn_{12}ac complex where the A_1 and A_2 tunneling states are formed from the $M = \pm 10$ states, corresponding to saturated magnetization along the S_4 anisotropy axis.[1a] Ising doublets with tunneling splitting have been also found for strongly anisotropic molecular wheels.[14b]

